

Regulation of biological tissue mineralization through post-nucleation shielding

Joshua C. Chang*

Mathematical Biosciences Institute, The Ohio State University, Columbus OH 43210

Robert M. Miura†

Department of Mathematical Sciences, New Jersey Institute of Technology, Newark NJ 07102

In vertebrates, insufficient availability of calcium and phosphate ions in extracellular fluids leads to loss of bone density and neuronal hyper-excitability. To counteract this problem, calcium ions are present at high concentrations throughout body fluids – at concentrations exceeding the saturation point. This condition leads to the opposite situation where unwanted mineral sedimentation may occur. Remarkably, ectopic or out-of-place sedimentation into soft tissues is rare, in spite of the thermodynamic driving factors. This fortunate fact is due to the presence of auto-regulatory proteins that are found in abundance in bodily fluids. Yet, many important inflammatory disorders such as atherosclerosis and osteoarthritis are associated with this undesired calcification. Hence, it is important to gain an understanding of the regulatory process and the conditions under which it can go awry. In this Letter, we use ideas from mean-field classical nucleation theory to study the regulation of sedimentation of calcium phosphate salts in biological tissues through the mechanism of post-nuclear shielding of nascent mineral particles by binding proteins. A critical concentration of regulatory protein is identified as a function of the physical parameters that describe the system.

PACS numbers: 82.60.-s, 82.39.-k, 87.15.R-, 87.10.Ed

In biology, ionic calcium (Ca^{2+}) plays many roles. Aside from its signaling duties, Ca^{2+} , along with inorganic phosphate ions (PO_4^-), are the main constituent of bones in vertebrates. For this reason, it is important for organisms to obtain adequate amounts of calcium from the environment. Under normal circumstances, Ca^{2+} is plentiful throughout extracellular spaces and in the circulatory system, stably existing in concentrations *exceeding* the saturation point, whereby sedimentation is favored. Even under the dangerous condition of hypocalcemia, Ca^{2+} may still be supersaturated relative to the most thermodynamically stable phase of calcium phosphate, hydroxyapatite (HAP), which is the building block of teeth and bones. Yet, while the deposition of calcium into bones is desirable, ectopic calcification into soft tissues is pathological and either causes or exacerbates a variety of inflammatory disorders including arteriosclerosis, heart disease, and arthritis [1–3]. So, the regulation of ectopic calcium sedimentation is important in maintaining the health of soft tissues.

When solutions are supersaturated with respect to HAP, it is formed in a multi-step process traversing through several intermediate mineral states. Although controversial, the first step in this process is thought to be formation of prenucleation clusters (PNC) [5], which are small complexes of approximately one Ca^{2+} per three PO_4^{3-} . These clusters aggregate in a calcium-dependent manner whereby they nucleate into spherical post-nucleation clusters composed of amorphous calcium phosphate (ACP) of molecular formula $\text{Ca}_2(\text{HPO}_4)_3^{2-}$. As long as supersaturation persists, and in the absence of regulation, ACP clusters continue to grow by absorbing additional “monomers” into its structure. By *monomer*

we refer to the small calcium phosphate building blocks of ACP, commonly thought to be so-called *Posner’s clusters*, with composition $\text{Ca}_9(\text{PO}_4)_6$. When the particles reach a particular size s_p , they sediment into the tissue.

This situation is seemingly incompatible with life as the persistent supersaturation of calcium and phosphate in biological fluids dictates continual sedimentation, at least in the absence of regulatory inhibition. Fortunately a regulatory mechanism does exist. The main machinery for preventing calcium phosphate sedimentation is the plasma protein fetuin-A (FA) [3, 6–9]. FA is an acidic protein that is found abundantly in blood as well as throughout all extracellular compartments. It interacts with the calcium phosphate mineralization process in several different ways. FA can directly bind calcium, with each molecule able to weakly and reversibly bind approximately 12–15 ions [10]. Yet, this direct binding of calcium is not the main regulatory mechanism of FA as it would effectively reduce the supersaturation. There is also evidence that FA binds to prenucleation clusters [8], although somewhat contradictory evidence has also shown that the presence of FA does not affect the rate of nucleation of calcium phosphate clusters [11]. Primarily, FA binds strongly to post-nuclear calcium-rich calcium-phosphate clusters, shielding them from further growth and imparting on them enhanced colloidal stability so that they do not sediment.

The combined process of mineralization and FA-induced inhibition is an example of a *nucleation* problem. Our approach to this problem is to use ideas from mean-field *classical nucleation theory* (CNT). It is notable, however, that theoretical treatments of the inherently high-dimensional stochastic problem of nucleation

also exist [12–14]. The mean-field theoretic CNT approach is ultimately motivated by the behavior of such stochastic treatments.

CNT explains the emergence and evolution of colloidal phases in solutions through the development of a simple thermodynamical picture. The key element of CNT is the assumption that the emergence of a new phase carries an energetic cost due to the creation of an interfacial surface. For a spherical cluster consisting of an integer number m monomer units with total surface area $s = (36\bar{v}^2\pi)^{1/3}m^{2/3}$, CNT assigns as per the *capillary approximation* the free energy

$$\Delta G/k_B T = \underbrace{\frac{\Delta G_\gamma}{\gamma s}} + \underbrace{\frac{\Delta G_\mu}{m\Delta\mu}} = \underbrace{\gamma s + \frac{\Delta\mu}{6\bar{v}\sqrt{\pi}} s^{3/2}}_{\text{spherical}}, \quad (1)$$

where $\Delta\mu$ is the molecular free energy per monomer in the cluster relative to in the solution (normalized by $k_B T$), \bar{v} is the volume per monomer, $\gamma > 0$ is the interfacial surface energy per unit area (normalized by $k_B T$). For constant supersaturation, $\Delta\mu < 0$ so that $\Delta G \rightarrow -\infty$ as $s \rightarrow \infty$, thereby thermodynamically favoring the existence of large clusters. Yet, as shown in Fig. 1(a), the state of pure-monomers ($s = 0$) is also a local minimum of this free energy. The emergence of clusters is governed by *kinetic* rather than thermodynamic considerations as an energy barrier of ΔG_{crit} corresponding to the free energy of a critical cluster with size s_* must be overcome. The steady-state mean-field rate at which clusters overcome this energy gap is exponential in the magnitude of the gap and is known as the Zeldovich rate

$$j_* = \kappa \exp\left(-\frac{\Delta G_{\text{crit}}}{k_B T}\right) \quad (2)$$

where κ is a constant with units of concentration per time. While the presence of prenucleation clusters in the calcium phosphate system violates the assumptions of CNT, Habraken et al. [5] showed that CNT is still applicable with the use of some minor modifications which result in the reduction of the effective energy gap ΔG_{crit} by an excess free energy ΔG_{ex} . Hence, we will assume for the purposes of this Letter that critically sized clusters of size s_* are forming spontaneously at some rate $j_* = \exp(-\Delta G_{\text{crit}} + \Delta G_{\text{ex}})$. In the blood and extracellular compartments, fluid is under constant exchange. For this reason, we will also assume that the supersaturation is constant, and hence that j_* and s_* are fixed, and study the growth of clusters after their nucleation.

Upon reaching size s_* , clusters are inclined to grow. Classical work by Landau, Lifshitz [15], have defined an advection problem to quantitatively describe this phase. This work has been extended throughout the years, and recently united with nucleation [16, 17], which is introduced as an effective boundary condition. We further extend this prior work by incorporating the effects of

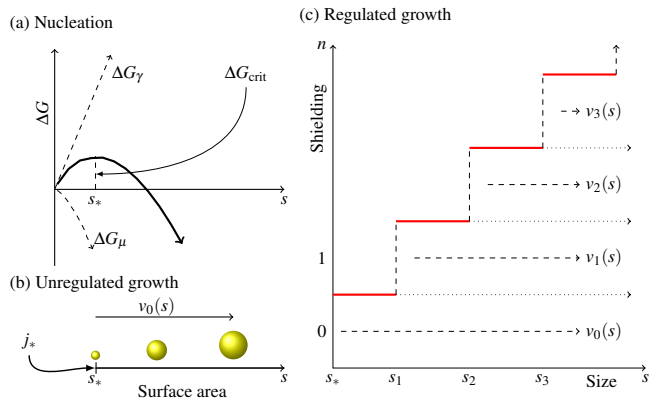


FIG. 1: Nucleation, growth, and shielding. (a) Classical nucleation of an initial critically-sized spherical mineral cluster of surface area s_* . The activation energy ΔG_{crit} corresponds to the energy of the premature cluster at a critical size s_* . A flux j_* of nucleating particles is generated by the system under the condition of supersaturation. (b) **Unregulated growth.** Upon nucleation, particles grow uncontrollably at a size dependent rate $v_0(s)$ as defined in Eq. 6. (c) **Regulated growth.** Shielding by n FA proteins modifies the effective growth rate of the mineral phase to v_n . Completely-shielded particles, where the surface area s is less than the shielding capacity s_n , do not grow.

shielding. Let ε be the thickness of the shielding layer, $\delta \gg \varepsilon$ be the thickness of the diffusion layer, r be the radius of the mineral phase of the cluster, and x be the radial coordinate extending from the center of the cluster. Our ultimate goal is to find the cluster volume growth rate $\dot{V} = \bar{v}J$ where \bar{v} is the effective monomer volume, and J is the flux of monomer units into the mineral phase. This flux, as shown in Fig. 2, is due to the balance of the competing surface reactions of absorption and dissolution and can be expressed as [17]

$$J = k_-(s - s') \left[\frac{\rho_r - \rho_s}{\rho_s} + \mathcal{O}(m^{-1/3}) \right], \quad (3)$$

where $s' \leq s$ is the surface area that is shielded, ρ_r is the monomer concentration directly at the interface of the mineral, k_- is the rate of the dissociation reaction per unit surface area, and ρ_s is the saturation concentration. The shielded surface area s' depends on the number of associated protein monomers. It takes certain values s_n , where the gaps between these values need not be uniform.

The concentration ρ_r depends on supply due to diffusion. We assume that mineral clusters are relatively immobile compared to both mineral monomers and FA protein. Outside of the shielding layer, the flux of monomers through a shell of radius $x > r + \varepsilon$ is described by Fick's law $J(x) = 4\pi x^2 D \partial_x \rho$ which implies that

$$J = 4\pi D \frac{(r + \delta)(r + \varepsilon)}{\delta - \varepsilon} (\rho_\infty - \rho_\varepsilon). \quad (4)$$

If we make the assumption that ε is small relative to the characteristic diffusion length, then the flux is determined by matching of Eq. 3 with Eq. 4 with $\rho_r \approx \rho_\varepsilon$.

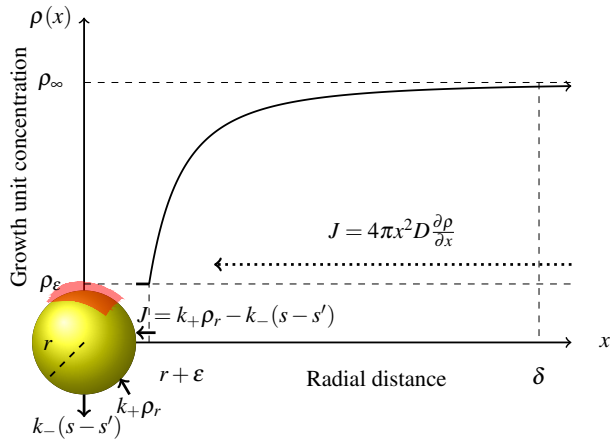


FIG. 2: Shielded diffusion-limited growth. FA protein forms a diffusion barrier of height ε and surface area $s' = s_n$, where n is the number of associated proteins, around the mineral cluster. The absorption rate $k_+\rho_r$ per unit surface area of the growth units depends on the local concentration ρ_r of growth units at the surface of the particle. Dissociation also occurs at rate k_- per unit surface area. Neither absorption nor dissociation occur in the shielded region (red). For ε sufficiently small, $\rho_r \approx \rho_\varepsilon$. The concentration ρ_r is then determined through conservation of flux. Outside of the diffusion layer (of thickness $\delta \gg r$), the concentration of growth units approaches ρ_∞ .

Combining Eq. 3 and Eq. 4, we arrive at the volume growth rate

$$\begin{aligned} \dot{V} &= \bar{v}J \approx k_-(s-s') \left[\frac{4\pi\bar{v}D(r+\varepsilon)(\rho_\infty - \rho_s)}{4\pi D(r+\varepsilon)\rho_s + k_-(s-s')} \right] \\ &\approx \frac{\alpha s^{1/2}(s-s')/\sqrt{16\pi}}{\omega s^{1/2} + (s-s')}, \end{aligned} \quad (5)$$

with lumped parameters $\omega = D\sqrt{4\pi}\rho_s/k_-$, and $\alpha = 8\bar{v}D\pi(\rho_\infty - \rho_s)$. In Eq. 5, we have also assumed that $\varepsilon \ll r$ and $(\delta - \varepsilon)/(\delta + r) \approx 1$. Note that in the limit as $s - s' \ll \omega s^{1/2}$, this growth rate is surface-limited, whereas in the limit as $s - s' \gg \omega s^{1/2}$, growth is diffusion limited. The parameter ω defines the length-scale under which surface-limited effects are significant. Typically, in nucleation problems, the surface-limited regime is ignored as it is only important when the particle is small. For the purposes of this system, however, the surface-limited effects can be significant regardless of the net particle size, particularly when the clusters are nearly-completely shielded. Furthermore, as particle size increases, the free surface area required to move into the diffusion-limited regime also increases. For more details on the derivation of these growth rates, please see the SUPPLEMENTAL METHODS.

Taking a continuum approach, one may describe the evolution of the concentration profile of clusters using an advection equation, where the cluster growth rate provides an effective “velocity” or drift. Overall, the dynamic concentration $c_n(s, t)$ of clusters of mineral surface area s associated with n FA monomers is described for all non-negative integers $n \geq 0$ for $s > s_n$ by the partial differential equations,

$$\frac{\partial c_n(s, t)}{\partial t} + \frac{\partial}{\partial s} \left[\overbrace{\frac{v_n(s)}{\omega s^{1/2} + (s - s_n)} c_n(s, t)}^{\text{diffusion limited}} - \lambda s^{1/2} (c_n(s, t) - c_{n-1}(s, t)) \right] = 0 \quad (6)$$

where $v_n(s)$ is surface growth rate dependent on the number of bound FA monomers, $s' = s_n$ for $n \geq 1$ and $s' = 0$ for $n = 0$, $\lambda = \sqrt{4\pi}D_{\text{FA}}\phi_\infty$, and for notational convenience we set $c_{-1}(s, t) \equiv 0$. The right-hand-side describes diffusion-limited shielding of the mineral particles by FA protein, which is assumed to have high affinity for the mineral phase (see SUPPLEMENTAL METHODS for details). The solution domain for Eq. 6 is shown in Fig. 1(c).

Similar to the approach of Farjoun and Neu [16], nucleation is included as an effective boundary condition due to flux balancing between the Zeldovich rate of Eq. 2, growth, and shielding. These considerations (see the SUPPLEMENTAL METHODS for details) lead to the effective boundary condition on the concentration of completely-unshielded clusters c_0 , so that

$$c_0^\infty(s_*) \equiv c_0(s_*, t) = \frac{j_*}{\lambda\sqrt{s_*} + \frac{\sqrt{4\pi}D(\rho_\infty - \rho_s)s_*^{3/2}}{\omega s_*^{1/2} + s_*}}. \quad (7)$$

Strictly speaking, the parameters ϕ_∞ and ρ_∞ contained in these expressions are themselves dynamical variables. Their evolution can be determined through mass conservation, as all changes are due to the balance between supply and consumption. We are interested however in the biologically-relevant situation where calcification is a local phenomenon coupled to global auto-regulatory processes that maintain supersaturation. For instance, fluid present in a knee joint is constantly replenished through interstitial flow. That is to say, we consider the heat-bath approximation of this system and set ϕ_∞ and ρ_∞ constant and examine the conditions for the regulation of sedimentation in this regime.

As detailed in the SUPPLEMENTAL METHODS, the PDE system of Eq. 6, provided Cauchy data $c_n(s, 0) = 0$ a.e., has the unique steady-state solution

$$c_n^\infty(s) = c_0^\infty(s_*) f_n^\infty(\sqrt{s}) \exp \left\{ -\frac{\lambda}{\alpha} \left[s \left(\omega + \frac{2}{3}\sqrt{s} \right) - s_* \left(\omega + \frac{2}{3}\sqrt{s_*} \right) \right] \right\} \quad (8)$$

where $c_0^\infty(s_*)$ is given by Eq. 7, and f_n^∞ are functions that obey a recursive integral relationship shown in the SUPPLEMENTAL METHODS. In particular, $f_0^\infty(\sqrt{s}) = \frac{(\omega + \sqrt{s})\sqrt{s_*}}{\sqrt{s}(\omega + \sqrt{s_*})}$.

The tapering of the solution has a characteristic length scale which is determined by the magnitude of λ/α , and hence, the concentration of FA. To inhibit sedimentation, at a minimum, the following condition on the concentration must hold:

$$\phi_\infty \gg \frac{3}{2} \frac{D}{D_{\text{FA}}} \frac{\bar{v}(\rho_\infty - \rho_s)}{s_*^{3/2}}. \quad (9)$$

$$R = \lambda\sqrt{s_*}c_0^\infty(s_*) + \sum_{n=0}^{\infty} \sum_{j=n}^{\infty} \frac{\lambda}{\sqrt{16\bar{v}^2\pi}} \int_{s_j}^{s_{j+1}} s c_n^\infty(s) ds = \lambda\sqrt{s_*}c_0^\infty(s_*) + \frac{\alpha c_0^\infty(s_*)}{\sqrt{16\bar{v}^2\pi}} \frac{s_*}{\omega + \sqrt{s_*}} + \mathcal{O}\left(\frac{\alpha^2}{\lambda^2}\right), \quad (11)$$

where the approximation is derived in the SUPPLEMENTAL METHODS in the regime where $\lambda s_1^{3/2} \gg \alpha$. R sets a minimum replenishment rate for new FA protein in order to maintain a steady concentration of FA, and hence colloidal stability. As seen in Eq. 7, the parameter λ comes into the denominator of $c_0^\infty(s_*)$. As a result, to the leading order, R increases as λ decreases. Failure to maintain this replenishment rate leads to decrease in ϕ_∞ , the concentration of FA. A drop in ϕ_∞ further decreases λ , thereby further exacerbating the situation (the more dilute the concentration, the more that is used). Thus, even a small destabilization in FA replenishment can feed-forward to avalanche into catastrophic calcium phosphate sedimentation. In this manner, the calcium phosphate regulatory system is yet another example of a biological system poised at criticality [18].

In this Letter we have utilized classical nucleation theory to provide a quantitative description of the growth of calcium phosphate nanoparticles interacting with a shielding protein. In contrast with other theoretical work on similar systems, we have not neglected possible surface-limiting regimes of the process. Our quantitative description of the process provides an estimate of the critical concentration of shielding protein necessary for stable long-term inhibition of calcification, as well as an estimate of the total rate that the protein is consumed. We also have found that any disruption of the ability to maintain the concentration of FA leads to *increased* overall consumption of the protein, and hence, exhaustion and sedimentation.

Acknowledgements – The authors would like to thank Lydia L. Shook (Yale School of Medicine), Tom Chou (UCLA Mathematics and Biomathematics), Huaxiong Huang (York University Mathematics), and Jonathan J.

Wylie (City University of Hong Kong Mathematics) for their comments and feedback relating to this work. This material is based upon work supported by the National Science Foundation under Agreement No. 0635561. JC also acknowledges support from the National Science Foundation through grant DMS-1021818, and from the Army Research Office through grant 58386MA.

$$f_n^\infty(\sqrt{s}) \sim (s - s_n + \omega\sqrt{s}) \frac{\sqrt{s_*}}{\omega + \sqrt{s_*}} \times \frac{1}{s_1} \prod_{j=1}^n \frac{\lambda[(s_j - s_{j-1})\sqrt{s_j} + s_j\omega]}{\lambda\omega s_j + \alpha}. \quad (10)$$

Using Eq. 10 along with Eq. 8, the total rate of FA protein consumption can be expressed as

Wylie (City University of Hong Kong Mathematics) for their comments and feedback relating to this work. This material is based upon work supported by the National Science Foundation under Agreement No. 0635561. JC also acknowledges support from the National Science Foundation through grant DMS-1021818, and from the Army Research Office through grant 58386MA.

* chang.1166@mbi.osu.edu

† miura@njit.edu

- [1] E. R. Smith, M. L. Ford, L. A. Tomlinson, C. Rajkumar, L. P. McMahon, and S. G. Holt, *Nephrology Dialysis Transplantation* **27**, 1957 (2012).
- [2] R. W. Bendon, in *Seminars in perinatology*, Vol. 20 (Elsevier, 1996) pp. 381–388.
- [3] L. Brylka and W. Jahnen-Dechent, *Calcified tissue international*, 1 (2013).
- [4] M. Salimi, J. Heughebaert, and G. Nancollas, *Langmuir* **1**, 119 (1985).
- [5] W. J. Habraken, J. Tao, L. J. Brylka, H. Friedrich, L. Bertinetti, A. S. Schenk, A. Verch, V. Dmitrovic, P. H. Bomans, P. M. Frederik, *et al.*, *Nature communications* **4**, 1507 (2013).
- [6] P. A. Price and J. E. Lim, *Journal of Biological Chemistry* **278**, 22144 (2003).
- [7] M. Herrmann, A. Kinkeldey, and W. Jahnen-Dechent, *Trends in Cardiovascular Medicine* (2012).
- [8] A. Heiss, V. Pipich, W. Jahnen-Dechent, and D. Schwahn, *Biophysical journal* **99**, 3986 (2010).
- [9] W. Jahnen-Dechent, A. Heiss, C. Schäfer, and M. Ketteler, *Circulation research* **108**, 1494 (2011).
- [10] M. Suzuki, H. Shimokawa, Y. Takagi, and S. Sasaki, *Journal of Experimental Zoology* **270**, 501 (1994).
- [11] C. N. Rochette, S. Rosenfeldt, A. Heiss, T. Narayanan, M. Ballauff, and W. Jahnen-Dechent, *Chembiochem* **10**,

- 735 (2009).
- [12] A. H. Marcus, *Technometrics* **10**, 133 (1968).
 - [13] M. R. D'Orsogna, B. Zhao, B. Berenji, and T. Chou, *The Journal of Chemical Physics* **139**, 121918 (2013).
 - [14] M. D'Orsogna, G. Lakatos, and T. Chou, *The Journal of chemical physics* **136**, 084110 (2012).
 - [15] I. M. Lifshitz and V. V. Slyozov, *Journal of Physics and Chemistry of Solids* **19**, 35 (1961).
 - [16] Y. Farjoun and J. C. Neu, *Physical Review E* **78**, 051402 (2008).
 - [17] Y. Farjoun and J. C. Neu, *Physical Review E* **83**, 051607 (2011).
 - [18] T. Mora and W. Bialek, *Journal of Statistical Physics* **144**, 268 (2011).

Symbol	Description
s	Surface area
m	Number of mineral monomers, where monomer refers to Posner's cluster $\text{Ca}_9(\text{PO}_4)_6$.
r	Radius
V	Volume
n	Number of shielding proteins
γ	Interfacial free energy per unit surface area
$\Delta\mu$	Chemical free energy per mineral monomer
ΔG	Gibbs free energy
$c_n(s, t)$	Concentration of mineral clusters of surface area s shielded by n FA monomers
s'	Shielded surface area
s_n	Amount of surface shielded (s') when n FA monomers are bound
δs	$s_{n+1} - s_n$ for $n \geq 1$
s_*	Critical cluster size at nucleation
s_p	Critical cluster size at sedimentation
D	Diffusivity of mineral monomers
D_{FA}	Diffusivity of FA monomers
k_-	Dissociation rate per unit surface area for mineral
ρ_∞	Concentration of mineral monomers
ρ_s	Saturation concentration
ϕ_∞	Concentration of FA monomers
\bar{v}	Mineral monomer volume
ω	$D\sqrt{4\pi\rho_s}/k_-$
α	$8\bar{v}D\pi(\rho_\infty - \rho_s)$
ε	Thickness of shielding layer (of FA protein)
λ	$\sqrt{4\pi D_{\text{FA}}\phi_\infty}$
k_B	Boltzman's constant
T	Temperature

TABLE S1: List of symbols used in the manuscript for easy reference

SUPPLEMENTAL METHODS

Growth rates

Growth of the mineral phase

Assuming that particles consist of spheres consisting of m subunit ‘‘monomers’’ each of volume \bar{v} , a m -mer has volume $V = \bar{v}m$ and surface area $s = (36\bar{v}^2\pi)^{1/3}m^{2/3}$. Given that some of its surface $s' \leq s$ is shielded, this particle experiences an instantaneous net flux of monomers into its structure due to the competition between absorption and dissociation

$$J = k_+\rho_r - k_-(s - s') \quad (\text{S1})$$

where ρ_r is the concentration of monomers at the surface, k_- is the dissociation rate per unit surface area, and k_+ is the absorption rate which is dependent on m as well as the free surface area (and can be related to k_-). There exists a critical concentration ρ_m at which a m -cluster is at equilibrium with its surroundings so that

$$k_+\rho_m - k_-(s - s') = 0. \quad (\text{S2})$$

At equilibrium, growth arrests, so the free energy gap between m and $m + 1$ also disappears so that,

$$\delta G/k_B T = \Delta\mu + (36\bar{v}^2\pi)^{1/3}\gamma((m+1)^{2/3} - m^{2/3}) = 0, \quad (\text{S3})$$

where $\Delta\mu = \log(\rho_s/\rho_m)$ is the normalized chemical potential. Eq. S3 implies that

$$\begin{aligned} \rho_m &= \rho_s \exp \left[(36\bar{v}^2\pi)^{1/3}\gamma((m+1)^{2/3} - m^{2/3}) \right] \\ &= \rho_s \left[1 + \gamma \left(\frac{32\bar{v}^2\pi}{3m} \right)^{1/3} + \mathcal{O}(m^{-4/3}) \right] \quad \text{as } m \rightarrow \infty. \end{aligned} \quad (\text{S4})$$

Eq. S4 together with Eq. S2 allows elimination of k_+ by substitution $k_+ = k_-(s - s')/\rho_m$ and implies that

$$\begin{aligned} J &= k_-(s - s') \\ &\times \left[\frac{\rho_r - \rho_s}{\rho_s} - \frac{\rho_r(32\bar{v}^2\pi/3)^{1/3}\gamma}{\rho_s m^{1/3}} + \mathcal{O}(m^{-2/3}) \right]. \end{aligned} \quad (\text{S5})$$

The concentration ρ_r is found through conservation of monomer mass by flux matching as in Fig. 2 in the quasi-steady diffusive limit, where the FA protein forms a shielding layer around the mineral of thickness ε . Outside of the shielding layer ($x > r + \varepsilon$), the monomer flux obeys Fick's law

$$\begin{aligned} J &= 4\pi x^2 D \partial_x \rho = 4\pi D \frac{(r + \delta)(r + \varepsilon)}{\delta - \varepsilon} (\rho_\infty - \rho_\varepsilon) \\ &= 4\pi D(r + \varepsilon)(\rho_\infty - \rho_\varepsilon) + \mathcal{O} \left(\frac{r + \varepsilon}{\delta - \varepsilon} \right), \end{aligned} \quad (\text{S6})$$

where the second equality is obtained by integration of the concentration from $x = r + \varepsilon$ to $x = r + \delta$, where $\delta \gg r$ is the thickness of the diffusion layer. At the surface, the flux is given by Eq. S5. Equating these fluxes while assuming that ε is small relative to the characteristic diffusion length ($\rho_r \approx \rho_\varepsilon$) allows us to solve for the monomer concentration at the mineral surface,

$$\rho_r \approx \rho_s \frac{4\pi D(r + \varepsilon)\rho_\infty + k_-(s - s')}{4\pi D(r + \varepsilon)\rho_s + k_-(s - s')}. \quad (\text{S7})$$

In Eq. S7, one sees that as $D \rightarrow \infty$, the concentration at r goes to ρ_∞ , as expected. Plugging this expression into Eq. S5 yields the growth law

$$\dot{V} = \bar{v}J \approx k_-(s - s') \left[\frac{4\pi\bar{v}D(r + \varepsilon)(\rho_\infty - \rho_s)}{4\pi D(r + \varepsilon)\rho_s + k_-(s - s')} \right]. \quad (\text{S8})$$

While clusters of any size can be shielded, shielded clusters below the size s_1 are not of our concern because they are inert. Hence, we only wish to find the shielded growth rate when $s > s_1$. Making the assumption that ε is small relative to $r > \sqrt{4\pi s_1}$, and substituting $r = \sqrt{s/4\pi}$, yields the volume growth rate in terms of s ,

$$\dot{V} = \frac{\alpha s^{1/2}(s - s')/\sqrt{16\pi}}{\omega s^{1/2} + (s - s')}, \quad (\text{S9})$$

with constants $\omega = D\sqrt{4\pi}\rho_s/k_-$, and $\alpha = 8\bar{v}D\pi(\rho_\infty - \rho_s)$. The surface area growth rate is related to the volume growth rate through the chain rule,

$$v_n(s) = \sqrt{\frac{16\pi}{s}} \dot{V} = \frac{\alpha(s - s_n)}{\omega s^{1/2} + (s - s_n)}. \quad (\text{S10})$$

Shielding rate

The shielding of the mineral phase by FA can be understood in a manner similar to the growth of the mineral phase. The overall adsorption rate of FA monomers onto the surface results from a balance between the diffusive supply and the surface reactions. Assuming first that mineral clusters have less mobility than FA, and letting the diffusivity of FA be D_{FA} , one may use similar reasoning as in the previous section to find that the flux of FA into the surface follows the relationship

$$\begin{aligned} J_{\text{FA}} &= k_{\text{on}}\phi_r(s - s') - k_{\text{off}}s' \\ &\approx D_{\text{FA}}\sqrt{4\pi}s(\phi_\infty - \phi_r), \end{aligned} \quad (\text{S11})$$

where k_{on} is the binding rate of FA to the mineral per unit free surface area per concentration, k_{off} is the dissociation rate of FA, ϕ_∞ is the far-field heat bath concentration of FA, and ϕ_r is the concentration at the surface. Eliminating the surface-concentration of FA, we find the overall rate

$$\begin{aligned} J_{\text{FA}} &= k_{\text{on}}(s - s') \frac{k_{\text{off}}s' + D_{\text{FA}}\phi_\infty\sqrt{4\pi}s}{k_{\text{on}}(s - s') + D_{\text{FA}}\sqrt{4\pi}s} \\ &\approx D_{\text{FA}}\phi_\infty\sqrt{4\pi}s, \end{aligned} \quad (\text{S12})$$

where we have assumed first that the unbinding reaction is slow relative to the binding reaction, and second, that the surface reactions are fast relative to diffusion.

Nucleation as a boundary condition

Critically-sized clusters (of size s_*) are assumed to be created at the Zeldovich rate j_* of Eq. 2. This rate is balanced with flux out due to growth and shielding. As in Farjoun and Neu [16], this growth flux is expressed in terms of the non-dimensional rate of number-growth, \dot{V}/\bar{v} of Eq. S9. So that,

$$j_* = \lim_{s \rightarrow s_*^+} \left[\left(D_{\text{FA}}\phi_\infty\sqrt{4\pi}s + \frac{\sqrt{4\pi}D(\rho_\infty - \rho_s)s^{3/2}}{\omega s^{1/2} + s} \right) c_0(s, t) \right]. \quad (\text{S13})$$

Hence, the combined effects of nucleation and shielding impose an effective boundary condition

$$c_0^\infty(s_*) \equiv c_0(s_*, t) = \frac{j_*}{\lambda\sqrt{s_*} + \frac{\sqrt{4\pi}D(\rho_\infty - \rho_s)s_*^{3/2}}{\omega s_*^{1/2} + s_*}}. \quad (\text{S14})$$

Nondimensionalization of PDE

We seek a convenient non-dimensionalization of our serial system of PDEs describing the shielded growth problem. We begin by normalizing the surface area s , which ranges between the critical nucleation surface area s_* and another critical surface area s_p which represents the surface area at sedimentation. Using these constants, we write the non-dimensionalized size variable

$$\hat{s} = \frac{s - s_*}{s_p - s_*} \quad (\text{S15})$$

critical cluster size s_* ,

$$\hat{s}_* = \frac{s_*}{s_p - s_*}, \quad (\text{S16})$$

shielded surface area,

$$\hat{s}' = \frac{s'}{s_p - s_*}, \quad (\text{S17})$$

and shielding levels $s' = s_n$,

$$\hat{s}_n = \frac{s_n}{s_p - s_*}. \quad (\text{S18})$$

Next, we define a new non-dimensionalized rate variable $\hat{\omega}$ such that

$$\hat{\omega} = \frac{\omega}{\sqrt{s_p - s_*}}. \quad (\text{S19})$$

The parameter $\hat{\omega}$ controls the transition between surface-limited and diffusion-limited-growth. This parameter is typically taken to be small, but it has been noted that such an assumption is not always good for real systems. We do not require $\hat{\omega}$ to be small for the purposes of our problem. Rescaling time

$$\hat{t} = \frac{\alpha t}{s_p - s_*} \quad (\text{S20})$$

results in the series of non-dimensional advection equations of asymptotically unit speed,

$$\frac{\partial \hat{c}_n}{\partial \hat{t}} + \frac{\partial}{\partial \hat{s}} \left[\frac{(\hat{s} + \hat{s}_* - \hat{s}_n) \hat{c}_n(\hat{s}, \hat{t})}{\hat{\omega}(\hat{s} + \hat{s}_*)^{1/2} + (\hat{s} + \hat{s}_* - \hat{s}_n)} \right] = -\hat{\lambda} \sqrt{\hat{s} + \hat{s}_*} (\hat{c}_n(\hat{s}, \hat{t}) - \hat{c}_{n-1}(\hat{s}, \hat{t})) \quad (\text{S21})$$

with non-dimensional shielding constant

$$\hat{\lambda} = \frac{\lambda(s_p - s_*)^{3/2}}{\alpha} \quad (\text{S22})$$

where the concentrations have been scaled by the nucleation boundary condition

$$\hat{c}_n(\hat{s}, \hat{t}) = \frac{c_n(s(\hat{s}), t(\hat{t}))}{c_0(s_*, t)}, \quad (\text{S23})$$

so that the concentration of critical clusters is fixed

$$\hat{c}_0(0, \hat{t}) = 1. \quad (\text{S24})$$

Solution of PDE system

The nondimensionalized partial differential equations of Eq. S21 can be solved serially by invoking the method of characteristics sequentially for each PDE. The solution to the PDEs contains the characteristic curves described by the equations

$$\frac{d\hat{s}}{d\hat{t}} = \frac{(\hat{s} + \hat{s}_* - \hat{s}')}{\hat{\omega}(\hat{s} + \hat{s}_*)^{1/2} + (\hat{s} + \hat{s}_* - \hat{s}')}. \quad (\text{S25})$$

The $\hat{s} - \hat{t}$ characteristics, as shown in Fig. 3, originate from points $(\hat{t}_0, \hat{s}(\hat{t}_0))$. They follow

$$\begin{aligned} \hat{t} - \hat{t}_0 &= \hat{s} - \hat{s}(\hat{t}_0) + 2\hat{\omega} \left[\sqrt{\hat{s} + \hat{s}_*} - \sqrt{\hat{s}(\hat{t}_0) + \hat{s}_*} \right] \\ &+ \hat{\omega} \hat{s}' \log \left(\frac{\sqrt{\hat{s} + \hat{s}_*} - \sqrt{\hat{s}'} \sqrt{\hat{s}(\hat{t}_0) + \hat{s}_*} + \sqrt{\hat{s}'}}{\sqrt{\hat{s} + \hat{s}_*} + \sqrt{\hat{s}'} \sqrt{\hat{s}(\hat{t}_0) + \hat{s}_*} - \sqrt{\hat{s}'}} \right). \end{aligned} \quad (\text{S26})$$

Particularly, for unshielded clusters where $\hat{s}' = 0$, the last line of Eq. S26 is zero.

Along these curves, the concentration varies as

$$\begin{aligned} \frac{d\hat{c}_n}{d\hat{t}} &= -\frac{\hat{\omega}}{2\sqrt{\hat{s} + \hat{s}_*}} \frac{\hat{s} + \hat{s}_* + \hat{s}'}{[\hat{\omega}\sqrt{\hat{s} + \hat{s}_*} + \hat{s} + \hat{s}_* - \hat{s}']^2} \hat{c}_n(\hat{t}) \\ &- \hat{\lambda} \sqrt{\hat{s} + \hat{s}_*} (\hat{c}_n(\hat{t}) - \hat{c}_{n-1}(\hat{s}, \hat{t})). \end{aligned} \quad (\text{S27})$$

For the purpose of solving these equations, it is advantageous to invoke the change-of-variables $u \equiv \sqrt{\hat{s} + \hat{s}_*}$, $\hat{s}' \equiv \hat{s}_n$, $ds = 2udu$, to reparameterize the curves as

$$\frac{d\hat{t}}{du} = 2u \left[\frac{\hat{\omega}u}{u^2 - \hat{s}_n} + 1 \right] \geq 0, \quad (\text{S28})$$

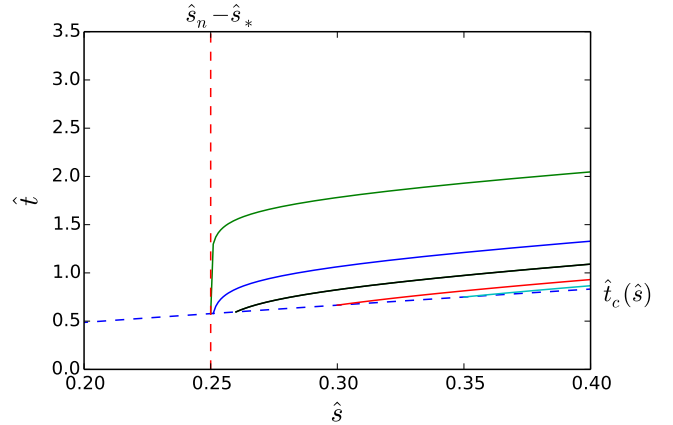


FIG. 3: Some sample $\hat{s} - \hat{t}$ characteristics for the PDE problem with $\hat{s}' = 0.25$. The characteristics emerge from the curve $\{(\hat{s}, \hat{t}_c(\hat{s}))\}$.

where it is evident that the relationship between \hat{t} and u is bijective. Hence, we may use u as a proxy for time, finding that the concentration profiles along these curves vary with u as

$$\begin{aligned} \frac{d\hat{c}_n}{du} &= - \left[\frac{\hat{\omega}}{u^2 - \hat{s}_n} \frac{u^2 + \hat{s}_n}{\hat{\omega}u + u^2 - \hat{s}_n} + 2\hat{\lambda}u^2 \frac{u^2 + \hat{\omega}u - \hat{s}_n}{u^2 - \hat{s}_n} \right] \hat{c}_n \\ &+ 2\hat{\lambda}u^2 \frac{u^2 + \hat{\omega}u - \hat{s}_n}{u^2 - \hat{s}_n} \hat{c}_{n-1}(\hat{s}(u), \hat{t}(u)). \end{aligned} \quad (\text{S29})$$

With the aid of an integrating factor, Eq. S29 can be written in the exact differential form

$$d \left\{ \frac{(u^2 - \hat{s}_n)^{\hat{\lambda}\hat{\omega}\hat{s}_n+1}}{u^2 + \hat{\omega}u - \hat{s}_n} \exp \left[\hat{\lambda}u^2 \left(\hat{\omega} + \frac{2}{3}u \right) \right] \hat{c}_n \right\} = 2\hat{\lambda}u^2 (u^2 - \hat{s}_n)^{\hat{\lambda}\hat{\omega}\hat{s}_n} \exp \left[\hat{\lambda}u^2 \left(\hat{\omega} + \frac{2}{3}u \right) \right] \hat{c}_{n-1}(u, \hat{t}(u)). \quad (\text{S30})$$

The solution for the unshielded particle concentration \hat{c}_0 corresponds to the homogeneous problem ($a = 0$; $\hat{c}_{-1} \equiv$

0). Respecting the boundary condition invoked by nucleation, as well as the initial Cauchy data, yields the solution

$$\hat{c}_0(\hat{s}, \hat{t}) = \frac{\hat{\omega} + \sqrt{\hat{s} + \hat{s}_*}}{\sqrt{\hat{s} + \hat{s}_*}} \frac{\sqrt{\hat{s}_*}}{\hat{\omega} + \sqrt{\hat{s}_*}} \frac{\exp\left[\hat{\lambda}\hat{s}_* \left(\hat{\omega} + \frac{2}{3}\sqrt{\hat{s}_*}\right)\right]}{\exp\left[\hat{\lambda}(\hat{s} + \hat{s}_*) \left(\hat{\omega} + \frac{2}{3}\sqrt{\hat{s} + \hat{s}_*}\right)\right]} H(\hat{t} - \hat{t}_c(\hat{s})), \quad (\text{S31})$$

where H is the unit step function and

$$\hat{t}_c(\hat{s}) = \hat{s} + 2\hat{\omega} \left(\sqrt{\hat{s} + \hat{s}_*} - \sqrt{\hat{s}_*} \right) \quad (\text{S32})$$

is analogous to a ‘‘first-passage-time’’ for the formation of size- \hat{s} clusters.

To solve for the subsequent concentrations, we take advantage of the Cauchy data by initializing all characteristic curves along the curve $(\hat{t}_c(\hat{s}), \hat{s})$ given by Eq. S32, thereby setting $\hat{c}_n = 0$ at the left endpoint. Hence, each point (\hat{s}, \hat{t}) such that $\hat{s} \geq \hat{s}' = \hat{s}_n$, and $\hat{t} \geq \hat{t}_c(\hat{s})$ lies uniquely on a single curve originating from

$$\sqrt{\hat{s}(\hat{t}_0) + \hat{s}_*} = \sqrt{\hat{s}' \frac{\sqrt{\hat{s} + \hat{s}_*} + \sqrt{\hat{s}'}}{\sqrt{\hat{s} + \hat{s}_*} - \sqrt{\hat{s}'}}} \exp\left[\frac{\hat{t} - \hat{s} - 2\hat{\omega}(\sqrt{\hat{s} + \hat{s}_*} - \sqrt{\hat{s}_*})}{\hat{\omega}\hat{s}'}\right] + 1 \\ \sqrt{\hat{s}' \frac{\sqrt{\hat{s} + \hat{s}_*} + \sqrt{\hat{s}'}}{\sqrt{\hat{s} + \hat{s}_*} - \sqrt{\hat{s}'}}} \exp\left[\frac{\hat{t} - \hat{s} - 2\hat{\omega}(\sqrt{\hat{s} + \hat{s}_*} - \sqrt{\hat{s}_*})}{\hat{\omega}\hat{s}'}\right] - 1. \quad (\text{S33})$$

As growth of the mineral phase occurs more quickly in the unshielded clusters than in the shielded clusters, the $\hat{s} - \hat{t}$ characteristics propagate more quickly in the unshielded clusters. Hence, the hierarchy holds

$$\text{supp}(\hat{c}_n) \subseteq \text{supp}(\hat{c}_{n-1}) \subseteq \dots \subseteq \text{supp}(\hat{c}_0). \quad (\text{S34})$$

In fact, the supports of all functions \hat{c}_n are equal, as necessitated by the coupling defined by the right-hand-side of Eq. S21. The creation of size- \hat{s} clusters of shielding n is driven more by the shielding of ‘‘ $n-1$ clusters’’ rather than the growth of ‘‘ n clusters.’’ We use this fact, along with the presence of an exponential term within the exact differential of the right hand side of Eq. S30 to formulate the ansatz

$$\hat{c}_n(\hat{s}, \hat{t}) = H(\hat{t} - \hat{t}_c(\hat{s})) \\ \times f_n(\hat{s}, \hat{t}) \exp\left[-\hat{\lambda}(\hat{s} + \hat{s}_*) \left(\hat{\omega} + \frac{2}{3}\sqrt{\hat{s} + \hat{s}_*}\right)\right], \quad (\text{S35})$$

where $f_n(\hat{s}, \hat{t})$ is a function such that $f_n(\hat{s}(\hat{t}_0), \hat{t}_c(\hat{s}(\hat{t}_0))) = 0$. Substitution of the ansatz into Eq S30, one finds that

along the characteristics,

$$f_n(u) = 2\hat{\lambda} \frac{u^2 + \hat{\omega}u - \hat{s}_n}{(u^2 - \hat{s}_n)^{\hat{\lambda}\hat{\omega}\hat{s}_n+1}} \\ \times \int_{\sqrt{\hat{s}(\hat{t}_0) + \hat{s}_*}}^u q^2 (q^2 - \hat{s}_n)^{\hat{\lambda}\hat{\omega}\hat{s}_n} f_{n-1}(q) dq, \quad (\text{S36})$$

where according to Eq. S31,

$$f_0(u) = \frac{\hat{\omega} + u}{u} \frac{\sqrt{\hat{s}_*}}{\hat{\omega} + \sqrt{\hat{s}_*}} \exp\left[\hat{\lambda}\hat{s}_* \left(\hat{\omega} + \frac{2}{3}\sqrt{\hat{s}_*}\right)\right]. \quad (\text{S37})$$

For solving $f_n(\hat{s}, \hat{t})$, the lower bound for the integral in Eq. S38 is taken from Eq. S33. For solving the next equation $f_{n+1}(\hat{s}, \hat{t})$, all instances of \hat{s}, \hat{t} are converted into u using Eq. S33.

Our interest is in long-term behavior of the system. In this regime, $\sqrt{\hat{s}(\hat{t}_0) + \hat{s}_*} \rightarrow \sqrt{\hat{s}'}$. Hence, we may write

$$f_n^\infty(u) = 2\hat{\lambda} \frac{u^2 + \hat{\omega}u - \hat{s}_n}{(u^2 - \hat{s}_n)^{\hat{\lambda}\hat{\omega}\hat{s}_n+1}} \\ \times \int_{\sqrt{\hat{s}_n}}^u q^2 (q^2 - \hat{s}_n)^{\hat{\lambda}\hat{\omega}\hat{s}_n} f_{n-1}^\infty(q) dq. \quad (\text{S38})$$

First, there is the question of whether these equations are well-posed. By the Cauchy-Schwarz inequality, one sees that

$$\int_{\sqrt{\hat{s}_n}}^u q^2 (q^2 - \hat{s}_n)^{\hat{\lambda}\hat{\omega}\hat{s}_n} f_{n-1}(q) dq \\ \leq \left[\int_{\sqrt{\hat{s}_n}}^u q^4 (q^2 - \hat{s}_n)^{2\hat{\lambda}\hat{\omega}\hat{s}_n} dq \right]^{1/2} \|f_{n-1}^\infty\|_{L^2(\sqrt{\hat{s}_n}, u)} \\ \leq \left[\frac{(u^2 - \hat{s}_n)^{4\hat{\lambda}\hat{\omega}\hat{s}_n+1}}{4\hat{\lambda}\hat{\omega}\hat{s}_n + 1} \right]^{1/4} \left[\frac{u^8 - \hat{s}_n^4}{8} \right]^{1/4} \|f_{n-1}^\infty\|_{L^2(\sqrt{\hat{s}_n}, u)}. \quad (\text{S39})$$

This computation gives us the pointwise bound on f_n^∞ ,

$$f_n^\infty(u) \leq \frac{2\hat{\lambda}}{(4\hat{\lambda}\hat{\omega}\hat{s}_n + 1)^{1/4}} \frac{u^2 + \hat{\omega}u - \hat{s}_n}{(u^2 - \hat{s}_n)^{3/4}} \\ \times \left[\frac{u^8 - \hat{s}_n^4}{8} \right]^{1/4} \|f_{n-1}^\infty\|_{L^2(\sqrt{\hat{s}_n}, u)}. \quad (\text{S40})$$

Using the fact that $f_0^\infty(u) = \mathcal{O}(1)$, it is easy to see that $f_n(u)$ is bounded and smooth for $u > \sqrt{\hat{s}_n}$, where it is of-note that f_n^∞ is bounded also in the vicinity of $\sqrt{\hat{s}_n}$.

Since the overall solution is tapered by the exponential term which goes as $s^{3/2}$, or as the volume, we are most interested in the behavior of $f_n^\infty(u)$ in the vicinity of $\sqrt{\hat{s}_n}$. In this limit, we use the binomial theorem to approximate the integrals of the general form

$$\begin{aligned} & \int_{\sqrt{\hat{s}_n}}^u q^2 (q^2 - \hat{s}_n)^{\hat{\lambda}\hat{\omega}\hat{s}_n} q^a (q^2 - \hat{s}_n)^b dq \\ &= \frac{\sqrt{\hat{s}_n^{a+1}}}{2} \int_0^{u^2 - \hat{s}_n} x^{\hat{\lambda}\hat{\omega}\hat{s}_n + b} \left(1 + \frac{x}{s_n}\right)^{(a+1)/2} dx \\ &= \frac{\sqrt{\hat{s}_n^{a+1}}}{2} \left[\frac{(u^2 - \hat{s}_n)^{\hat{\lambda}\hat{\omega}\hat{s}_n + b + 1}}{\hat{\lambda}\hat{\omega}\hat{s}_n + b + 1} + \mathcal{O}\left((u^2 - \hat{s}_n)^{\hat{\lambda}\hat{\omega}\hat{s}_n + b + 2}\right) \right]. \end{aligned} \quad (\text{S41})$$

Eq. S41 allows us to evaluate f_1^∞ to the leading order

$$f_1^\infty(u) \sim \frac{\sqrt{\hat{s}_*}}{\hat{\omega} + \sqrt{\hat{s}_*}} \frac{\hat{\lambda}(\sqrt{\hat{s}_1} + \hat{\omega})}{\hat{\lambda}\hat{\omega}\hat{s}_1 + 1} [(u^2 - \hat{s}_1) + \hat{\omega}u]. \quad (\text{S42})$$

Through an inductive argument, one finds that for $n \geq 1$,

$$\begin{aligned} f_n^\infty &\sim (u^2 - s_n + \hat{\omega}u) \frac{\sqrt{\hat{s}_*}}{\hat{\omega} + \sqrt{\hat{s}_*}} \\ &\times \frac{1}{\hat{s}_1} \prod_{j=1}^n \frac{\hat{\lambda}((\hat{s}_j - \hat{s}_{j-1})\sqrt{\hat{s}_j} + \hat{s}_j\hat{\omega})}{\hat{\lambda}\hat{\omega}\hat{s}_j + 1}. \end{aligned} \quad (\text{S43})$$

We retain both $u^2 - s_n$ and $\hat{\omega}u$ in this expression because it is unclear which term is large. As n increases however, the $\hat{\omega}u$ term will begin to dominate.

Rate of FA consumption

Since we know the rate of protein association as a function of n and s , we can compute the total rate of FA consumption. Denote R_{jk} the cumulative rate of minimal consumption in shielding particles of j FA monomers with size $s \in (s_k, s_{k+1})$. We derive this rate first for the shielding of unshielded clusters of size at most s_1 , R_{00} . Returning back to an integer parameterization of the size,

$$m(s) = s^{3/2} / \sqrt{36\bar{v}^2\pi},$$

where we will call the inverse mapping $s(m)$, it is clear that the total rate of consumption of FA for these clusters follows

$$R_{00} = \sum_{m=m(s_*)}^{m(s_1)} \lambda \sqrt{s(m)} c_0^\infty(s(m)). \quad (\text{S44})$$

The sum in Eq. S44 can be approximated by a left-Riemann integral so that

$$\begin{aligned} & \sum_{m=m(s_*)}^{m(s_1)} \lambda \sqrt{s(m)} c_0^\infty(s(m)) \approx \\ & \int_{m(s_*)}^{m(s_1)} \lambda \sqrt{s(m)} c_0^\infty(s(m)) dm. \end{aligned} \quad (\text{S45})$$

After transformation from m back to s , one finds that

$$R_{00} = \frac{\lambda}{\sqrt{16\bar{v}^2\pi}} \int_{s_*}^{s_1} s c_0^\infty(s) ds. \quad (\text{S46})$$

Generalizing this result, it is easy to see that

$$R_{nj} = \frac{\lambda}{\sqrt{16\bar{v}^2\pi}} \int_{s_j}^{s_{j+1}} s c_n^\infty(s) ds. \quad (\text{S47})$$

The total consumption rate of FA protein follows

$$\begin{aligned} R &= \overbrace{\lambda \sqrt{s_*} c_0^\infty(s_*)}^{\text{at nucleation}} + \sum_{n=0}^{\infty} \sum_{j=n}^{\infty} R_{nj} \\ &= \lambda \sqrt{s_*} c_0^\infty(s_*) + \frac{\lambda}{\sqrt{16\bar{v}^2\pi}} \sum_{n=0}^{\infty} \int_{s_n}^{\infty} s c_n^\infty(s) ds, \end{aligned} \quad (\text{S48})$$

where the first term represents FA consumed in the instantaneous shielding of critical clusters. At this point we will attempt to find the behavior of R , for large values of $\lambda s_1^{3/2} \gg \alpha$. We apply Laplace's method to find that

$$\sum_{j=n}^{\infty} R_{nj} \sim \frac{\alpha}{\sqrt{16\bar{v}^2\pi}} \sum_{n=0}^{\infty} \frac{s_n f_n^\infty(s_n) \exp\left\{-\frac{\lambda}{\alpha} s_n \left(\omega + \frac{2}{3}\sqrt{s_n}\right)\right\}}{(\omega + \sqrt{s_n}) \exp\left\{-\frac{\lambda}{\alpha} s_* \left(\omega + \frac{2}{3}\sqrt{s_*}\right)\right\}}. \quad (\text{S49})$$

Now, to compute Eq. S48, it only remains to sum over the indices n in Eq. S49. As before, we construct a Riemann integral and apply Laplace's method to obtain

$$\begin{aligned} \sum_{n=1}^{\infty} \sum_{j=n}^{\infty} R_{nj} &\approx \frac{\alpha}{\delta s \sqrt{16\bar{v}^2\pi}} \int_{s_1}^{\infty} \left\{ \frac{s f_n^\infty(s)}{(\omega + \sqrt{s})} \right. \\ &\times \left. \frac{\exp\left\{-\frac{\lambda}{\alpha} s \left(\omega + \frac{2}{3}\sqrt{s}\right)\right\}}{\exp\left\{-\frac{\lambda}{\alpha} s_* \left(\omega + \frac{2}{3}\sqrt{s_*}\right)\right\}} \right\} ds \\ &\sim \frac{\alpha^2}{\lambda \delta s \sqrt{16\bar{v}^2\pi}} \frac{s_1 f_1^\infty(s_1) \exp\left\{-\frac{\lambda}{\alpha} s_1 \left(\omega + \frac{2}{3}\sqrt{s_1}\right)\right\}}{(\omega + \sqrt{s_1})^2 \exp\left\{-\frac{\lambda}{\alpha} s_* \left(\omega + \frac{2}{3}\sqrt{s_*}\right)\right\}}. \end{aligned} \quad (\text{S50})$$

We will handle the $n = 0$ case differently as its solution is of a different form. Application of Laplace's method yields

$$\sum_{j=0}^{\infty} R_{0j} \sim \frac{\alpha c_0^\infty(s_*)}{\sqrt{16\bar{v}^2\pi}} \frac{s_*}{\omega + \sqrt{s_*}}, \quad (\text{S51})$$

which outside of the $c_0^\infty(s_*)$ term is $\mathcal{O}(\lambda^0)$. Hence, for large values of λ , the dominant consumer of FA monomers is unshielded clusters of size less than s_1 .